Neurobiology of Aging 80 (2019) 29–37

Contents lists available at ScienceDirect

Neurobiology of Aging

journal homepage: www.elsevier.com/locate/neuaging

Layer-specific axonal degeneration of serotonergic fibers in the prefrontal cortex of aged A53T α-synuclein–expressing mice

Jeanette Wihan [a,*], Janina Grosch [a], Liubov S. Kalinichenko [b], Christian P. Müller [b], Jürgen Winkler [a,*], Zacharias Kohl [a,*]

[a] Department of Molecular Neurology, Friedrich-Alexander University Erlangen-Nürnberg, Erlangen, Germany
[b] Section of Addiction Medicine, Department of Psychiatry and Psychotherapy, Friedrich-Alexander University Erlangen-Nürnberg, Erlangen, Germany

ARTICLE INFO

Article history:
Received 11 September 2018
Received in revised form 25 February 2019
Accepted 23 March 2019
Available online 1 April 2019

Keywords:
Parkinson's disease
Alpha-synuclein
Serotonin
Prefrontal cortex
Serotonin transporter

ABSTRACT

Axonal pathology precedes dopaminergic cell loss in Parkinson's disease (PD), indicating a dying back axonopathy of nigrostriatal projections. Although most attention focused on the dopaminergic system, increasing evidence implies a compromised serotonergic system in PD as well. By combining immunohistological and biochemical approaches, a profound layer-specific reduction of the serotonergic input to the prefrontal cortex (PFC) layers II and V/VI in aged mutant A53T α-synuclein–expressing mice (A53T mice) was detected. In addition, the altered fiber network was characterized by swollen axons and enlarged axonal varicosities within all PFC layers, but most pronounced in PFC layer I. Although prefrontal serotonin levels and synaptic protein expression were preserved, aged A53T mice showed increased levels of kinesin family member 1a and vesicular monoamine transporter 2. Together with increased tryptophan hydroxylase 2 mRNA levels in the raphe nuclei and an elevated serotonin receptor 1b expression in the PFC, these findings point to compensatory mechanisms within the serotonergic system to overcome the reduced neuritic input to the PFC in this transgenic animal model for PD.

1. Introduction

Aging is the most important risk factor for developing Parkinson's disease (PD) (Driver et al., 2009). Although the progressive loss of dopaminergic midbrain neurons is an important structural hallmark in PD, human *postmortem* analyses suggest an early degeneration of striatal dopaminergic axons that may precede neuronal cell loss. This conclusion is consistent with findings in human, indicating that the extent of dopaminergic cell loss in the substantia nigra is often exceeded by the profound loss of striatal dopaminergic terminals (reviewed in Cheng et al., 2010). In line, a severe reduction by 31%–61% of putaminal dopaminergic axons without changes in the density of tyrosine hydroxylase–positive nigral neurons was observed in patients with early-stage PD compared with age-matched controls (Chu et al., 2012). However, disease heterogeneity and *postmortem* delay may significantly affect the outcome of *postmortem* studies. Thus, several transgenic and virus-induced animal models were generated to address the challenging question whether the initial pathogenic event occurs within the axon terminals and thereby precedes neuronal cell loss in terms of a "dying back" mechanism. Although none of these models is able to mimic the full range of pathological features of PD, important insights into pathophysiological changes have been generated that further support the notion of an early axonopathy in PD (reviewed in Tagliaferro and Burke, 2016). Intriguingly, at the onset of motor symptoms in patients with PD, the majority of striatal terminals (50%–80%) are already lost (Cheng et al., 2010), implying a long-lasting premotor phase in PD. Compensatory mechanisms are considered to maintain brain functions over years from the onset of synaptic degeneration to the first symptoms, thus masking the underlying neurodegenerative processes. The further decline of neuronal functions combined with a failure or exhaustion of compensatory mechanisms may determine the onset of symptoms.

Although the dopaminergic system has attracted major attention in PD, a substantial body of evidence suggests the involvement of other monoaminergic neurotransmitter systems, particularly, the serotonergic system (Barone, 2010). Indeed, serotonergic neurons in the raphe nuclei are affected early by Lewy body pathology at Braak stage 2 (Braak et al., 2003) and *postmortem* analysis revealed a profound loss of serotonergic neurons in PD brains (Halliday et al., 1990). Serotonin (5-hydroxytryptamine [5-HT]) synthesis takes

* Corresponding authors at: Department of Molecular Neurology, Friedrich-Alexander University Erlangen-Nürnberg, Schwabachanlage 6, D-91054 Erlangen, Germany. Tel.: +49 9131 85 39324; fax: +49 9131 85 36597.
E-mail addresses: jeanette.wihan@uk-erlangen.de (J. Wihan), juergen.winkler@uk-erlangen.de (J. Winkler), zacharias.kohl@fau.de (Z. Kohl).

0197-4580/$ – see front matter © 2019 Elsevier Inc. All rights reserved.
https://doi.org/10.1016/j.neurobiolaging.2019.03.014

place in serotonergic neurons within the raphe nuclei expressing tryptophan hydroxylase 2 (Tph2), the rate-limiting enzyme for 5-HT synthesis (Walther et al., 2003). To process 5-HT for subsequent release, the vesicular monoamine transporter 2 (vMAT2) drives packaging of cytosolic 5-HT into presynaptic storage vesicles (Kelly, 1993; Narboux-Nême et al., 2011). Prior to packaging, vesicle precursors loaded with the small GTPase Rab3A and a variety of soluble N-ethylmaleimide-sensitive-factor attachment receptor (SNARE) fusion proteins are transported from the neuronal soma to the presynaptic compartment (reviewed in Rizzoli, 2014). The anterograde transport within axons is predominantly mediated by the kinesin motor protein family, in particular the kinesin family member 1a (Kif1a; Vale, 2003). Upon packaging and neuronal activation, 5-HT is released into the extracellular space binding to different 5-HT receptors at postsynaptic and presynaptic membranes. Finally, residual 5-HT within the synaptic cleft is rapidly taken up into presynaptic terminals by the serotonin transporter (SERT), thus maintaining a stable 5-HT pool that is available for subsequent release (Iversen, 2000).

The prefrontal cortex (PFC), composed of 6 discrete layers with excitatory pyramidal neurons (80%–90%) and inhibitory GABAergic interneurons (Ascoli et al., 2008; Riga et al., 2014), receives an extensive serotonergic input (Linley et al., 2013), predominantly provided by the dorsal raphe nuclei (DRN). Intriguingly, human *postmortem* analyses demonstrated a profound reduction of prefrontal 5-HT levels in patients with PD (Scatton et al., 1983), whereas in vivo imaging studies detected diminished SERT binding in the PFC of patients at an intermediate stage of PD (Politis et al., 2010). Linked to important psycho-emotional and cognitive functions (Arango et al., 2002, Carter et al., 2005, Liy Salmeron and Meneses, 2008), alterations within the prefrontal 5-HT system may contribute in particular to some of the nonmotor symptoms in PD.

Intraneuronal aggregation of α-synuclein (α-syn) is a well described neuropathological feature in PD (Braak et al., 2003) and is considered to play an important role in the pathogenesis of the disease. Thus, we aimed at investigating the impact of α-syn on the prefrontal serotonergic system. Therefore, a detailed PFC layer-specific analysis of the serotonergic innervation and axonal pathology in aged PDGF-hA53T-synuclein-transgenic mice (A53T mice) was undertaken. These mice express the human A53T mutant α-syn under the neuron-specific platelet-derived growth factor β (PDGFβ) promoter (Hashimoto et al., 2003). To better characterize the prefrontal serotonergic system, we biochemically analyzed 5-HT levels, synaptic protein, and 5-HT receptor expression as well as the expression of vesicle packaging and transport proteins in 52-week-old A53T mice compared with control littermates.

2. Material and methods

2.1. Animals and tissue processing

Transgenic 52-week-old mice expressing human A53T mutant α-syn under the control of the PDGFβ promoter (Hashimoto et al., 2003) and corresponding age-/gender-matched non-transgenic (non-tg) littermates were kept group-housed under a 12-h light-dark cycle with free access to food and water. All experiments were carried out in accordance with the guidelines of international standards for the care and use of laboratory animals and were approved by the local governmental commission for animal health. Before tissue processing, 52-week-old mice were perfused transcardially with a 0.9% sodium chloride solution under deep anesthesia. For biochemical analysis, brains were removed, snap-frozen, and prefrontal cortices as well as raphe tissue were dissected semi-frozen. For immunohistological analyses, the hemispheres were divided and postfixed in 4% paraformaldehyde overnight. Tissues were cryoprotected in 30% (w/v) sucrose and 0.1 M sodium phosphate solution (pH 7.4) and cut sagittally into 40-μm-thick sections using a sliding microtome.

2.2. Immunostaining

For α-syn immunohistochemistry, free-floating sections were incubated with 0.6% H_2O_2 (30 minutes) to quench endogenous peroxidase activity. After citrate buffer treatment (14 minutes, 87 °C) and blocking (3% donkey serum, 0.3% Triton X-100, 2 h), free-floating sections were incubated for 5 days at 4 °C with following primary antibodies: rat anti-human α-syn (1:20; Enzo Life Sciences, Lörrach, Germany) and mouse anti-rodent/human α-syn (1:500; BD Bioscience, San Jose, CA, USA). Chromogenic immunodetection was conducted by combining a donkey anti-rat or donkey anti-mouse biotinylated secondary antibody (1:1000; Dianova, Hamburg, Germany) with the avidin-biotin-peroxidase complex (1:500; Vector Laboratories, Burlingame, CA, USA) before diaminobenzidine incubation. For immunofluorescent co-stainings, the H_2O_2 quenching step was omitted. After antigen retrieval and blocking, sections were incubated with the respective primary antibodies for 72 h at 4 °C: rabbit anti-SERT (1:2000; ImmunoStar, Hudson, WI, USA), goat anti-5-HT (1:1000; ImmunoStar), and rat anti-Ctip2 (COUP-TF-interacting protein 2; 1:500; Abcam, Cambridge, UK). Secondary antibodies were donkey-derived, species-specific and conjugated with Alexa-488 (1:1000; Life Technologies, Carlsbad, CA, USA), Alexa-647, or Rhodamine Red-X (1:1000; Dianova). 4',6-Diamidine-2'-phenylindole dihydrochloride (1:10,000; Sigma, St. Louis, MO, USA) was used as a nuclear counterstain.

2.3. Microscopy and quantification

2.3.1. Qualitative analysis of α-syn expression

Regional expression of human and total α-syn was assessed using a Zeiss Imager M2 microscope. Images were taken with equal exposure time. The expression pattern was visualized by imaging whole brain sections with 2.5-fold magnification using the Virtual Tissue Compiler tool of the Stereo Investigator software (Stereo-investigator 10.04; MicroBrightField, Williston, VT, USA).

2.3.2. Quantification of SERT+ fibers and varicosities within the PFC

Fiber length of SERT+ neurites within the PFC was determined in sagittal sections at 0.475 mm lateral of the midline (according to Paxinos & Franklin's mouse brain atlas, Paxinos and Franklin, 2012) by analyzing confocal image stacks (20 slices, 9.5 μm thickness, 0.5 μm interval, 1024 × 1024) acquired on a ZEISS LSM 780 confocal scanning laser microscope (63× PL APO oil objective, pinhole corresponding to 1 Airy unit). Three regions of interest (x/y 84.26 μm) were chosen, matching the cortical layers I, II, and V/VI. Ctip2 staining was analyzed to visualize neurons residing in cortical layers V and VI. For quantification, 2 confocal image stacks per cortical layer and animal were analyzed using the open source plugin "simple neurite tracer" of ImageJ 1.49p (Longair et al., 2011). Two-dimensional visualization of serotonergic innervation was conducted by converting z-stacks of traced fibers into line stacks, followed by the generation of two-dimensional projections using the "GroupedZ projector" tool (ImageJ 1.49p). The total number, size, and distribution of SERT+ varicosities within the PFC were assessed in identical confocal image stacks by converting image stacks into maximum intensity projections using the ImageJ software. After background subtraction, automated counting of varicosities was performed using the ImageJ plugin "Analyze particles". To select for varicosities, morphological criteria were implemented by thresholding for a minimum size of 1 μm^2 and a circularity of

0.3–1 as previously described (Nayyar et al., 2009).Two maximum intensity projections per animal and cortical layer were analyzed.

2.4. Protein isolation and Western blot analysis

Mice were sacrificed, and the PFC was subdivided from dissected brains. To separate proteins belonging either to the soluble or membrane fraction, sequential protein extraction was performed as previously described (Nuber et al., 2013). Briefly, tissues were homogenized, and proteins from the soluble and membrane fraction were separated using TBS + (50 mM Tris/HCl; pH 7.4; 175 mM NaCl, 5 mM EDTA), protease inhibitor (Roche, Basel, Switzerland) and TBS+ containing 1% Triton X-100. Each extraction step was followed by ultracentrifugation (20 minutes, 120,000 × g, 4 °C). For Western blot analysis, protein concentrations were determined using the bicinchoninic acid protein assay kit (Thermo Scientific, Waltham, MA, USA), and 10 μg (TBS + soluble/cytosolic) or 8 μg (TBS+/TX100 soluble/membrane) of protein was run on 4%–12% Bis-Tris gels (Invitrogen, Life Technologies, Carlsbad, CA, USA) before blotting on polyvinylidene fluoride membranes that are optimized for fluorescence detection systems (Millipore, Burlington, VT, USA). After blocking for 1 h in 1% bovine serum albumin diluted in PBS-T (phosphate buffered saline supplemented with 0.1% Tween-20), membranes were probed with the following primary antibodies overnight at 4 °C: rat anti-human α-syn (1:100; Enzo Life Sciences), mouse anti-rodent/human α-syn (1:100; BD Bioscience), rabbit anti-5-HT 1b receptor (1:500; Santa Cruz, Dallas, TX, USA), rabbit anti-5-HT 1a receptor (1:500; Abcam), mouse anti-5-HT 2c receptor (1:500; Santa Cruz), mouse anti-Kif1a (1:1000; BD Bioscience), mouse anti-dynein (1:1000; Millipore), rabbit anti-vMAT2 (1:1000; Alomone, Jerusalem, Israel), mouse anti-PSD-95 (postsynaptic density protein 95; 1:500; Abcam), rabbit anti-synapsin 1 (1:1000; SySy, Göttingen, Germany), mouse anti-Rab3a (1:10,000; SySy), goat anti-SNAP-25 (1:500; Santa Cruz), mouse anti-synaptophysin (1:500; Abcam), rabbit-anti-β actin (1:1000; Abcam), mouse anti-GAPDH (glyceraldehyde-3-phosphate dehydrogenase; 1:10,000; Millipore), and rabbit anti-Pan-Cadherin (1:1000; Abcam). After washing in phosphate buffered saline, membranes were incubated with donkey-derived secondary antibodies conjugated with Alexa-488 (1:1000; Life Technologies) or Alexa-647 (1:1000; Dianova). Signal capture was conducted using a Fusion FX7 detection system (Peqlab/VWR, Erlangen, Germany), and quantification of signal intensities was performed using the Bio1D software (Vilber Lourmat). Levels of cytosolic proteins residing in the soluble fraction were normalized to GAPDH or the cytoskeletal protein β actin, whereas levels of membrane-associated proteins were normalized to Pan-Cadherin, a ubiquitously expressed group of transmembrane proteins.

2.5. Quantitative real-time PCR

Total RNA was extracted from raphe tissue using QIAzol Lysis Reagent (Qiagen, Venlo, Netherlands) for tissue homogenization. Upon homogenization, phase separation was induced by adding chloroform and subsequent centrifugation. RNA was purified using the RNeasy mini kit according to the manufacturer's instructions (Qiagen), and RNA concentration was determined using the NanoDrop technology (Peqlab/VWR). cDNA was generated using the GoScript Reverse Transcription System (Promega, Madison, WI, USA), and gene transcription was quantified on a LightCycler 480 system (Roche, Basel, Switzerland) using the SSo Fast EvaGreen Supermix (Bio-Rad, Hercules, CA, USA). Primers: Tph2 (5′-TCTA CACCCCG GAACCAGAT-3′; 5′- GCAAAGGCCGAACT CGATTG-3′) house-keeping genes: β3 tubulin (5′-TAGACCCCAGCGGCAACTAT-3′; 5′-GTTCCAGGTTCCAAGTCCACC-3′), Pgk1 (5′-GTC GTGATGAGGG TGGACTT-3′; 5′-AACCGACTTGGCTCCATTGT-3′), Hprt (5′-GTCATGTC ACCCT AGTCC-3′; 5′-GCAAGT CTTTCAGTCCTGTCC-3′).

2.6. Analysis of 5-HT levels in the PFC

Measurement of 5-HT within the PFC was performed using high-pressure liquid chromatography (HPLC). Two distinct groups of 52-week-old A53T mice and non-tg littermates were perfused, and PFCs were dissected as described previously. Samples containing 500 pg dihydroxybenzylamine as an internal standard were analyzed by HPLC using electrochemical detection. The column used was an ET 125/2, Nucleosil 120-5, C-18 reversed phase column (Macherey-Nagel, Düren, Germany). The mobile phase consisted of 75 mM NaH2PO4, 4 mM KCl, 20 mM EDTA, 1.5 mM SDS, 100 mL/L diethylamine, 12% methanol, and 12% acetonitrile and was adjusted to pH 6.0 using phosphoric acid. The electrochemical detector was set at 500 mV versus an ISAAC reference electrode (Antec, Zoeterwoude, Netherlands) at 30 °C (Amato et al., 2011). To combine analyses obtained in 2 separate HPLC runs, 5-HT levels of individual samples were normalized to the mean 5-HT levels of each batch.

2.7. Statistical analyses

Statistical analyses were performed, and the respective graphs were obtained using Prism 6.0 (GraphPad Software, San Diego, CA, USA). Data were presented as mean ± standard error of the mean. Statistical outliers were detected using the "robust regression and outlier removal" method (ROUT; Q = 1%) (Motulsky and Brown, 2006), and differences between means were analyzed using two-tailed Student's t-test, if not indicated differently; p-values < 0.05 were considered to be statistically significant ($^{*} = p < 0.05$; $^{**} = p < 0.01$).

3. Results

3.1. Expression of human transgenic A53T α-syn

To examine the regional expression pattern of human α-syn in the A53T mouse model, we assessed whole-brain sagittal sections of 52-week-old A53T and non-tg mice. Immunostainings revealed a pronounced expression of the transgene within the PFC, thalamus, olfactory bulb, and hippocampus of A53T mice (Fig. 1A, upper panel). Moreover, the expression pattern of human transgenic α-syn closely resembled the expression of endogenous rodent α-syn in non-tg mice as shown with antibodies specific for either human α-syn only or rodent and human α-syn (total α-syn). The assessment of α-syn protein levels in 8 brain regions confirmed a pronounced expression within the PFC, the olfactory bulb, and the thalamus of A53T mice (Fig. 1A, lower panel). In contrast, moderate expression levels of human α-syn were observed in the ventral and dorsal hippocampus. No expression of human α-syn was detected in non-tg mice.

Given the widespread expression of transgenic α-syn within the PFC of A53T mice, we aimed at evaluating the level of total α-syn within this region. A 1.6-fold increase of total α-syn was observed in A53T mice compared with non-tg animals ($^{*}p = 0.024$; $t = 2.766$; $df = 8$; Fig. 1B, left panel). Furthermore, we confirmed the profound expression of transgenic α-syn in the PFC of A53T mice using immunofluorescent stainings (Fig. 1B, left and right panel, respectively).

3.2. Reduced serotonergic innervation and axonal beading in A53T mice

Because transgenic α-syn is not only present in serotonergic raphe neurons and their hippocampal projections (Deusser et al.,

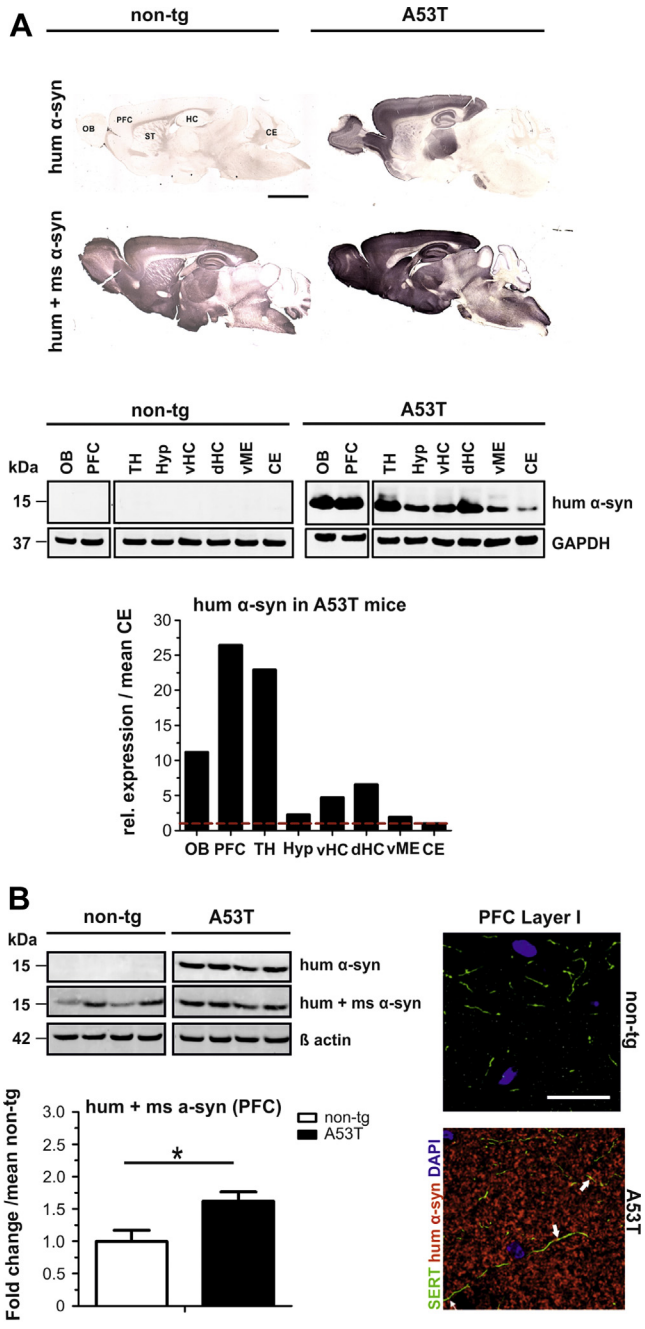

Fig. 1. Expression of human A53T α-syn in the PFC of A53T mice. (A) Sagittal brain sections of transgenic A53T mice showing the expression pattern of human α-syn in the OB, PFC, HC, and TH, scale bar = 200 μm. Western blot analysis of brain subregions confirmed the immunohistochemically identified expression pattern of human α-syn. Note the prominent expression within the PFC of A53T mice (n = 2). (B) Brain tissue was sequentially extracted to resolve cytosolic proteins, and prefrontal α-syn expression was quantified. Human A53T α-syn was strongly expressed within the PFC of A53T mice (Western blot left panel, confocal images right panel, scale bar = 20 μm). The quantification of total α-syn (human + mouse) revealed significantly increased total α-syn levels in A53T compared with non-tg littermates (n = 5, $^{*}p < 0.05$; left panel). Note the spatial proximity of serotonergic fibers expressing the SERT and transgenic human α-syn (right panel, white arrows). Abbreviations: α-syn, α-synuclein; CE, cerebellum; dHC, dorsal hippocampus; HC, hippocampus; Hyp, hypothalamus; non-tg, non-transgenic; OB, olfactory bulb; PFC, prefrontal cortex; SERT, serotonin transporter; TH, thalamus; vHC, ventral hippocampus; vME, ventral mesencephalon.

2015), but also highly expressed within the PFC of A53T mice, we asked whether α-syn overexpression might have an impact on the serotonergic innervation of the PFC. SERT+ fibers provided a layer-specific innervation to the PFC with an intense innervation of the superficial layer I as well as the deeper layers V and VI and a sparse innervation of layers II and III (Fig. 2A/2B). More importantly, A53T mice showed a 1.6-fold reduction in the total length of SERT+ fibers in the PFC layer II ($^{**}p = 0.002$; t = 4.695; df = 8) and a 1.8-fold reduction in the PFC layers V/VI ($^{*}p = 0.016$; t = 3.026; df = 8) compared with non-tg mice. Interestingly, the innervation by serotonergic fibers in PFC layer I remained unchanged ($p = 0.601$; t = 0.544; df = 8; Fig. 2C).

In addition, morphological analysis of SERT+ fibers in the PFC of transgenic mice revealed thick and intensely stained axons as well as fibers with enlarged varicosities (Fig. 3A; white arrows). Although the total number of varicosities was comparable between the groups, the percentage of very large (>9 μm^2) varicosities was significantly increased in A53T mice in all PFC layers (layer I: $^{**}p = 0.006$; t = 3.708; df = 8; layer II: $^{*}p = 0.039$; t = 2.462; df = 8; layer V/VI: $p = 0.036$; t = 2.515; df = 8; Fig. 3B/C). In addition, an increased density of large (6–9 μm^2) varicosities was seen in PFC layer I ($^{*}p = 0.012$; t = 3.213; df = 8; Fig. 3C). Intriguingly, 5-HT staining highly colocalized with the enlarged SERT+ varicosities (Fig. 4A), but we did not detect any differences in overall 5-HT levels in PFC tissue measured with HPLC ($p = 0.821$; t = 0.233; df = 10; Fig. 4B). In addition, we analyzed protein levels of distinct synaptic proteins directly involved in synaptic release of 5-HT. Although a 1.3-fold increase of the presynaptic protein Rab3a ($^{*}p = 0.013$; t = 3.031; df = 10) was observed in the PFC of aged A53T animals, protein levels of the presynaptic proteins synapsin 1, SNAP-25 as well as synaptophysin, and the postsynaptic protein PSD-95 remained unchanged (Fig. 4C).

3.3. Increased Tph2 expression in the raphe and elevated protein expression of vesicle transport and packaging proteins in the PFC of A53T mice

Given the significant loss of prefrontal serotonergic fibers without alterations of 5-HT levels, we hypothesized that potential age-dependent compensatory mechanisms overcome the loss of serotonergic fibers within the PFC of aged A53T mice. Hence, we determined Tph2 mRNA expression in raphe tissue of A53T and non-tg mice and observed a 6.6-fold increase of Tph2 expression in the raphe of A53T mice (Mann-Whitney *U*-test $^{*}p = 0.0159$, Fig. 5A). In addition to 5-HT biosynthesis, we analyzed the expression of proteins involved in vesicle transport and packaging in the PFC of these mice. Indeed, protein levels of Kif1a, which is mainly involved in the anterograde axonal transport of synaptic vesicle precursors, were increased in aged A53T mice (Mann Whitney U, $^{*}p = 0.035$), whereas the expression of the retrograde motor protein dynein remained unchanged ($p = 0.219$; t = 1.320; df = 9; Fig. 5B). Furthermore, we investigated the expression of vMAT2 playing a crucial role in the uptake and storage of cytosolic monoamines, including 5-HT, within synaptic vesicles. Again, we observed a significantly higher expression of vMAT2 within the PFC of A53T mice than non-tg mice ($^{**}p = 0.006$; t = 3.527; df = 9; Fig. 5B), suggesting not only an augmented transport of vesicle precursors to the terminals but also an increased uptake of 5-HT into these vesicles.

3.4. Increased 5-HT 1b receptor expression in the PFC of A53T mice

The expression of serotonergic autoreceptors on serotonergic neurons provides an intrinsic feedback mechanism in the regulation of 5-HT synthesis and release. Thus, we further assessed the membrane localization of the inhibitory 5-HT 1b receptor, present as both autoreceptor and heteroreceptor in the PFC. Notably, the membrane localization of 5-HT 1b was 1.8-fold increased in the PFC of aged A53T mice ($^{**}p = 0.007$; t = 3.359; df = 10; Fig. 5C). In

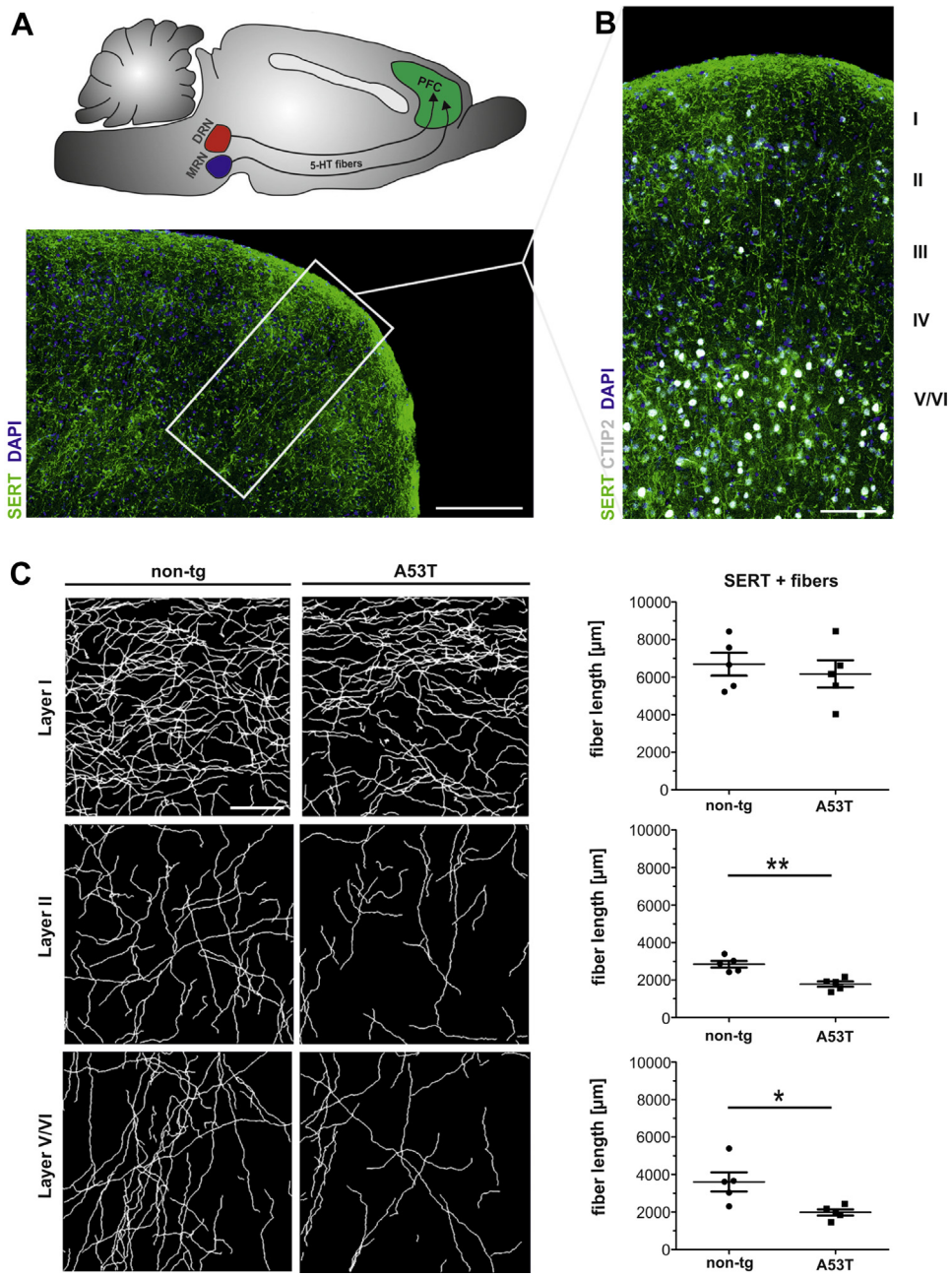

Fig. 2. Reduced serotonergic innervation of the PFC in aged A53T mice. (A) Illustration of the rodent brain depicting the serotonergic innervation of the PFC. Serotonergic fibers originate from the brainstem median (MRN, blue) and dorsal raphe nuclei (DRN, red). A confocal tile scan displays widespread serotonergic innervation (SERT, green) of the PFC, lower panel, scale bar = 200 µm (A/B). Note the dense innervation of cortical layer I and deeper layers V/VI, right panel: scale bar = 100 µm. (C) Representative 2D projections and quantification of traced SERT+ fibers revealed a significantly reduced serotonergic innervation of PFC layers II and V/VI in A53T mice, scale bar = 20 µm (n = 5, $^{*}p < 0.05$, $^{**}p < 0.01$). Abbreviations: non-tg, non-transgenic; PFC, prefrontal cortex; SERT, serotonin transporter.

contrast, the expression of 5-HT 1a and 5-HT 2c heteroreceptors was not altered ($p = 0.28$ and $p = 0.33$, respectively).

4. Discussion

To closely mirror human pathology in PD, transgenic mouse models have been generated either expressing human wild-type α-syn or mutant α-syn linked to sporadic or familial PD. Indeed, most of these models are able to recapitulate important neuropathological features of the disease; however, potential limitations need to be critically evaluated. The A53T mice ("line 8"; Hashimoto et al., 2003) express human A53T α-syn under regulatory control of the PDGFβ promoter leading to a progressive neuronal accumulation of α-syn in the forebrain, in particular in the neocortex, the hippocampus, and the olfactory bulb. Overall, this expression pattern closely resembles the reported neuronal expression of PDGFβ in the rodent brain (Sasahara et al., 1992). Initially described by Masliah et al. (2000), mice overexpressing human wild-type α-syn under the PDGFβ promoter showed neuronal inclusions particularly in deeper layers of the neocortex, the CA3 region of the hippocampus, and the olfactory bulb as well as a progressive loss of dopaminergic terminals in the basal ganglia associated with a late-onset motor deficit.

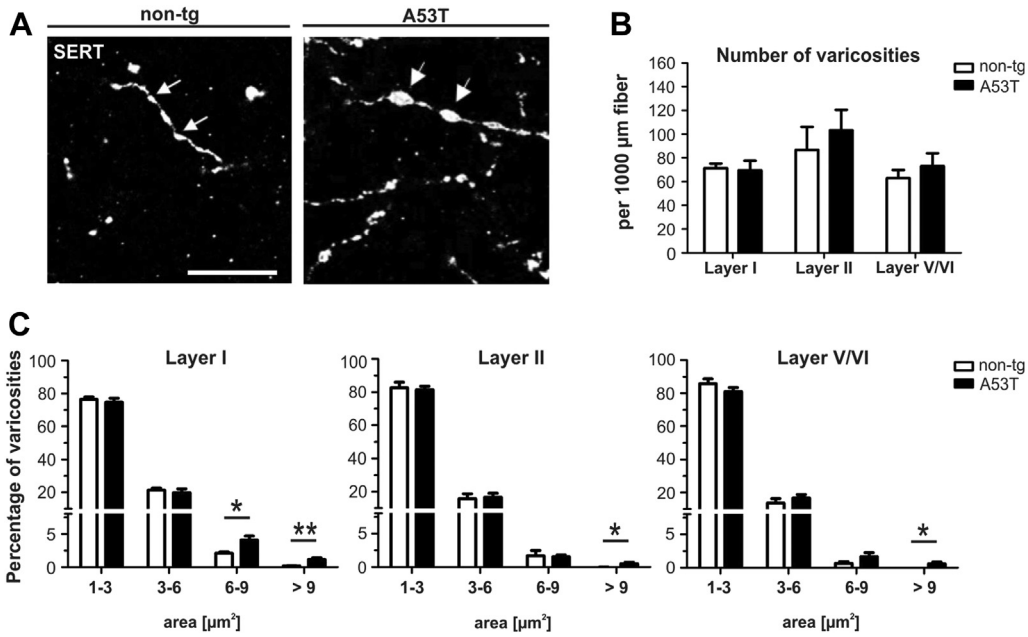

Fig. 3. Overexpression of human A53T α-syn affects axonal morphology of serotonergic neurites. (A) Representative confocal images show an altered morphology of SERT+ fibers (white) in PFC layer I with enlarged varicosities (arrows) in A53T mice, scale bar = 10 µm. (B) Total number of varicosities and size distribution (C) was assessed by analyzing maximum intensity projections of 2 chosen regions of interest per layer and animal. Although the total number of varicosities was similar between groups, the percentage of large varicosities was significantly increased in A53T mice (n = 5, * $p < 0.05$, ** $p < 0.01$). Abbreviations: α-syn, α-synuclein; non-tg, non-transgenic; SERT, serotonin transporter.

Structurally, α-syn is highly conserved among vertebrates, differing in 6 amino acids between human and murine α-syn (Lavedan, 1998). Although linked to familial PD in humans, the A53T mutation in patients corresponds to the wild-type sequence of murine α-syn. However, mice overexpressing the human A53T variant under the PDGFβ promoter developed a severe neurodegenerative and behavioral phenotype (Hashimoto et al., 2003). Moreover, hippocampal neurogenesis defects (Kohl et al., 2012; Winner et al., 2008) and a reduction of serotonergic fibers in the dorsal dentate gyrus have been identified in A53T mice (Deusser et al., 2015). Although this animal model recapitulates several important hallmarks of sporadic PD, such as the slowly progressive and age-dependent accumulation of α-syn, the structural and functional defects of the striatal dopaminergic system, as well as the late-onset of motor impairments, the spatial expression of α-syn in A53T mice differs to some extent from the regions with increased α-syn aggregation in patients with sporadic PD. Although the PDGFβ promotor drives α-syn expression in the neocortex and hippocampus and rather to a lower degree in the brainstem, human *postmortem* studies of Lewy pathology in PD indicate an early involvement of the brainstem, followed by a caudorostral progression toward cortical regions (Braak et al., 2003). Thus, the predominant accumulation of α-syn in cortical projection areas of serotonergic neurons might locally favor the onset of neurite degeneration at this site, whereas accumulation within the raphe neurons may play a less prominent role in this animal model. However, the A53T mouse model still represents a powerful tool to study the potential pathogenic role of α-syn and thus has the potential to reveal important insights into the vulnerability of monoaminergic systems. In addition, it is worth noting that under physiological baseline conditions expression levels of α-syn mRNA in mice and humans are low in subcortical regions and the brainstem, but high in the neocortex and limbic systems (Rockenstein et al., 2001). Confirming the preferential forebrain expression pattern, we identified a profoundly increased expression of human α-syn in the PFC of A53T mice. Considering the pathogenic role of α-syn, we hypothesized that an increased accumulation within the PFC interferes with the extrinsic innervation by serotonergic fibers, thereby providing novel hints toward an increased vulnerability of serotonergic terminals. Consistent with the physiological abundance of endogenous α-syn in presynaptic terminals (Burré, 2015), we observed a profound and punctate-like immunoreactivity of human α-syn protein in the neuropil throughout the PFC of A53T mice. Because the widespread accumulation of α-syn is not restricted to the serotonergic system, it is important to note that structural changes may not be exclusively linked to an accumulation within serotonergic terminals but related to the local micromilieu of the prefrontal neuritic network.

Although the innervation by serotonergic fibers was preserved in the superficial PFC layer I of aged A53T mice, we observed a profound layer-specific reduction of SERT+ fibers in PFC layer II and V/VI. Notably, a reduced serotonergic innervation was already reported in the PFC of human PD brains (Azmitia and Nixon, 2008). However, a layer-specific analysis of the innervation has not been performed yet. The PFC receives serotonergic input from two distinct types of axon terminals: fine-caliber smooth axons (D-type) arising from the DRN and M-type terminals with large spherical varicosities arising from the median raphe nuclei (Hornung et al., 1990; Kosofsky and Molliver, 1987). In contrast to cortical layers II-V which are predominantly innervated by D-type fibers, large beaded M-fibers are primarily observed in cortical layer I (Wilson and Molliver, 1991). Thus, a restricted loss of serotonergic fibers within PFC layer II and V/VI might indicate an increased fiber-type–specific vulnerability of D-type fibers due to α-syn expression. Similar differences in the fiber-type–specific vulnerability were observed in rodent models after administration of the neurotoxin 3,4-methylenedioxymethamphetamine (Molliver et al., 1990). However, underlying mechanisms contributing to this distinct fiber-type–specific vulnerability are not yet well understood. Recently, we reported a distinct subregional loss of serotonergic fibers within the hippocampus of aged A53T mice, affecting the dorsal part of the dentate gyrus infrapyramidal blade while sparing the ventral part of the infrapyramidal and suprapyramidal blades (Deusser et al., 2015). Although the hippocampus is known to be predominantly innervated by the median raphe nuclei

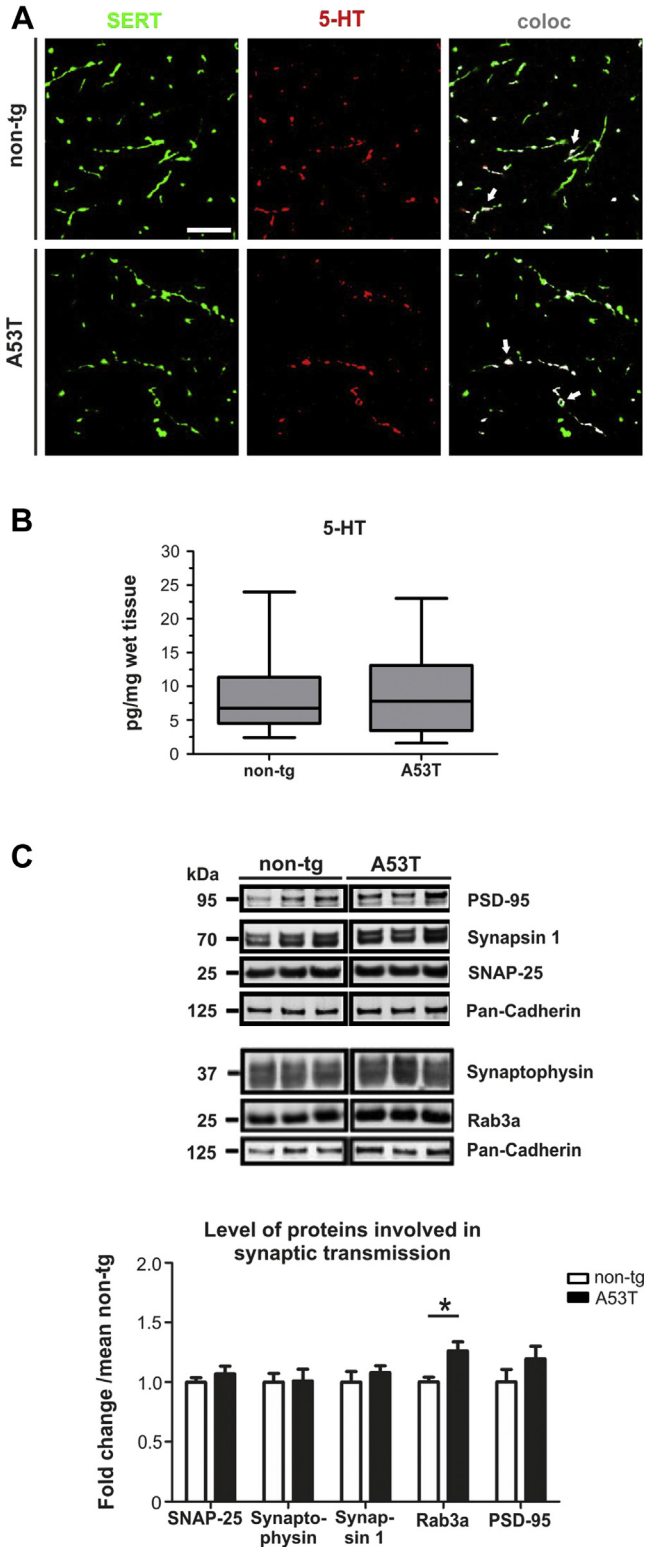

Fig. 4. No alterations in prefrontal serotonin (5-HT) levels but increased Rab3a expression. (A) Confocal images revealed the main localization of 5-HT (red) within SERT+ (green) varicosities (white arrows, scale bar = 10 μm). (B) Determined (high-pressure liquid chromatography) 5-HT levels in dissected PFCs were similar between groups (non-tg, n = 14; A53T, n = 15). (C) Western blot analysis revealed an increased expression of the presynaptic protein Rab3a in the PFC of A53T mice (n = 6, $^*p < 0.05$), whereas protein levels of the presynaptic proteins synapsin 1, SNAP-25, synaptophysin, and the postsynaptic protein PSD-95 remained unchanged. Abbreviations: α-syn, α-synuclein; 5-HT, 5-hydroxytryptamine; non-tg, non-transgenic; SERT, serotonin transporter.

(Muzerelle et al., 2016), a detailed analysis of changes in the sub-regional innervation by M-type or D-type fibers is missing so far.

Postmortem studies reported an increased loss of serotonergic neurons within the DRN of depressed PD patients (Paulus and Jellinger, 1991). However, no loss of serotonergic neurons was present in aged A53T mice (Deusser et al., 2015), which suggests a retrograde axonal degeneration of prefrontal serotonergic terminals that precedes neuronal cell loss in the raphe nuclei. Similarly, a profound loss of dopaminergic axons in the striatum that preceded dopaminergic cell loss was observed following viral expression of human A53T α-syn in rats (Chung et al., 2009). Notably, axonal loss was accompanied by the occurrence of dystrophic dopaminergic axons, characterized by swollen and bulging axons. A similar axonal phenotype was observed in the PFC of A53T mice. Determining the size of SERT+ varicosities revealed a significantly higher proportion of enlarged varicosities in the PFC of A53T compared with non-tg mice. Swollen axons with enlarged varicosities are common in many neurodegenerative diseases, and similar changes were also found in prefrontal serotonergic fibers in patients with PD (Azmitia and Nixon, 2008). Moreover, the presence of dystrophic serotonergic neurites has been associated with aging (Van Luijtelaar et al., 1989). Anatomical examination of aged Wistar rats revealed aberrant serotonergic fibers within the frontoparietal cortex already at the age of 12 months before serotonergic fiber loss became apparent at the age of 18 months (Van Luijtelaar et al., 1989). Based on these findings, it was proposed that the appearance of morphologically aberrant fibers is the first indication of degeneration during aging. Because aging is the most prominent risk factor for developing PD (Driver et al., 2009), age-related changes in the prefrontal serotonergic system might contribute early to the pathogenesis in PD. Despite a prominent reduction in the density of serotonergic fibers, prefrontal 5-HT levels were not decreased, suggesting that an increased 5-HT content in the preserved serotonergic terminals compensates the serotonergic deficit in the compromised network. Increasing evidence supports a preclinical phase preceding the onset of symptoms in PD. Although still under debate, the duration of this preclinical phase in patients with PD has been estimated to last for years or even decades (Hawkes, 2008). Particularly, compensatory mechanisms within monoaminergic neurotransmitter systems have been presumed to contribute to this long preclinical stage. However, the compensatory potential appears to be limited. Although 5-HT levels in the PFC of A53T mice were unaffected, prefrontal 5-HT levels in patients with PD are reduced (Scatton et al., 1983). These findings suggest a fine-tuned threshold during disease progression that is exceeded once the degeneration predominates over compensatory mechanisms. Vice versa, increased 5-HT synthesis may reflect early compensatory changes that take place to overcome incipient degeneration. Indeed, we identified increased mRNA levels of Tph2, the rate-limiting enzyme for 5-HT synthesis, within the raphe of aged A53T mice as well as an increased prefrontal protein level of the motor protein Kif1a mediating anterograde transport of synaptic vesicle precursors to axonal terminals. Moreover, we detected an increased expression of the vesicle packaging protein vMAT2 mainly involved in the packaging of monoamines into synaptic vesicles thereby reducing cytosolic monoamine levels. This sequestering machinery may be important for neuronal survival because free cytosolic monoamines are prone to oxidation resulting in reactive harmful species (Chen et al., 2008). Besides increased 5-HT synthesis, 5-HT may accumulate within axonal terminals because of synaptic dysfunctions interfering with neurotransmitter release. Recently, two independent studies reported a profound reduction of synapsin 1 in the rodent whole brain and hippocampal lysates following α-syn overexpression (Kohl et al., 2016; Nemani et al., 2010). Synapsins play a major role in synaptic vesicle trafficking and are required for proper synaptic neurotransmission. In aged A53T mice, we did not observe any changes in the prefrontal

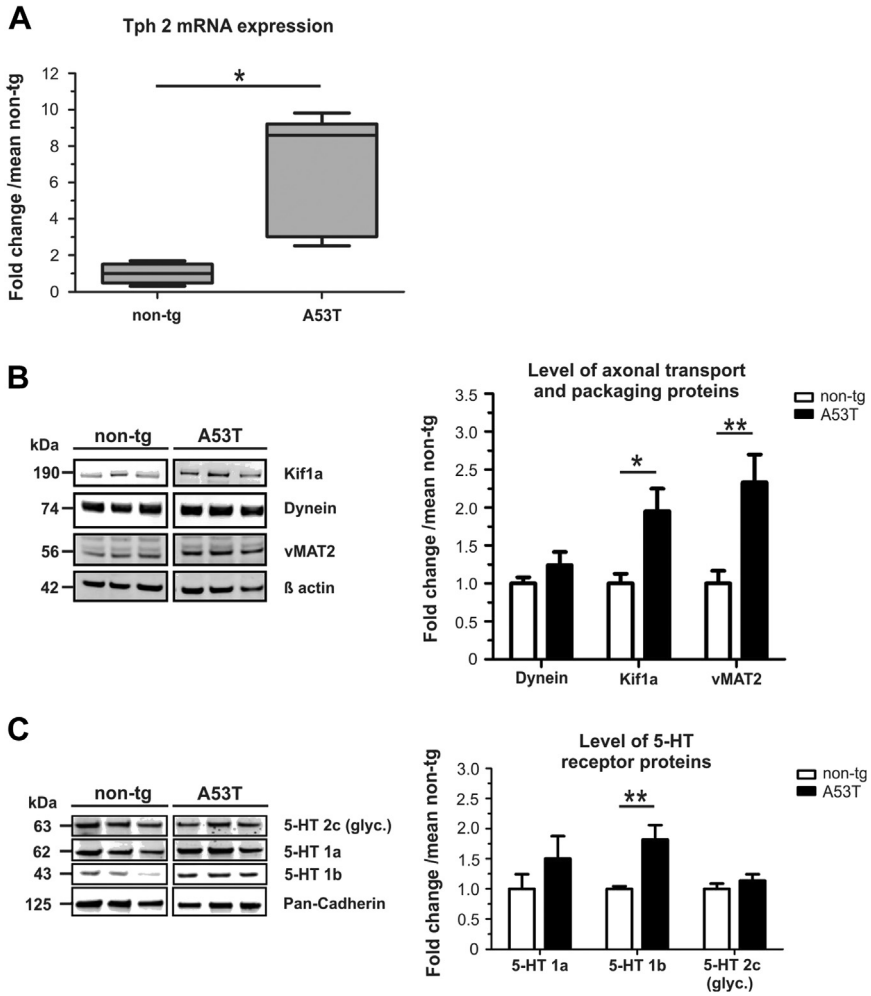

Fig. 5. Increased Tph2 expression in the raphe of A53T mice is accompanied by increased prefrontal levels of the anterograde motor protein Kif1a, the vesicle packaging protein vMAT2, and the 5-HT 1b receptor. (A) Quantitative real-time PCR revealed an increased Tph2 expression in the raphe of A53T mice (non-tg, n = 5; A53T, n = 6; Mann-Whitney *U*-test). (B) Expression of the anterograde motor protein Kif1a was markedly increased in A53T mice, whereas the expression of the retrograde motor protein dynein was similar between groups. Note the striking increase of vesicular monoamine transporter 2 (vMAT2) in A53T mice (non-tg, n = 6; A53T, n = 5). (C) Prefrontal protein levels of the 5-HT 1b receptor were considerably increased in A53T compared with non-tg mice. In contrast, levels of 5-HT 1a and 5-HT 2c receptors were not different (n = 6). * $p < 0.05$, ** $p < 0.01$. Abbreviations: α-syn, α-synuclein; 5-HT, 5-hydroxytryptamine; non-tg, non-transgenic; SERT, serotonin transporter; Tph2, tryptophan hydroxylase 2.

expression of synapsin 1, SNAP-25, synaptophysin or the postsynaptic protein PSD-95. However, we detected an increased protein expression of the small GTPase Rab3a, involved in the recruitment of synaptic vesicles to the active zone (Leenders et al., 2001).

5-HT synthesis and release is controlled by the activation of 5-HT autoreceptors on serotonergic neurons. Although the expression of 5-HT 1a autoreceptors is restricted to the raphe nuclei, 5-HT 1b autoreceptors are mainly located at serotonergic axons and terminals across the forebrain (Riad et al., 2000). Importantly, an involvement of the 5-HT 1b receptor in the modulation of 5-HT reuptake has been suggested (Daws et al., 2000; Hagan et al., 2012). This is of particular interest because active 5-HT uptake, mediated via SERT, is essential to constrain the duration and spatial effect of released 5-HT. Thus, an increased expression of 5-HT 1b receptors in the PFC of aged A53T mice might be an important response to restrict 5-HT signaling more stringently.

5. Conclusion

Despite a profound layer-specific reduction of the serotonergic input to the PFC and the aberrant morphology of residual axons, prefrontal 5-HT levels were not affected in aged A53T mice. However, we observed an upregulation of Tph2 expression in the raphe nuclei of A53T mice accompanied by an increased prefrontal expression of proteins involved in anterograde vesicle transport, vesicle packaging, and neurotransmission. Together, these results point toward compensatory responses within the serotonergic system to overcome the reduced input to the PFC. Similar alterations in the nigrostriatal system have been reported after dopamine depletion (reviewed in Blesa et al., 2017). Although the precise pathophysiological mechanisms remain unclear, compensatory mechanisms within the monoaminergic neurotransmitter systems may help to prolong the asymptomatic preclinical phase in PD. Therefore, improving our knowledge of compensatory mechanisms in PD will be important for the development of disease-modifying therapies even before the onset of PD-related symptoms.

Disclosure

The authors declare no conflict of interest.

Acknowledgements

This work was supported by the University Hospital Erlangen (ELAN MN-12-08-06-1-Kohl), Germany, the Deutsche

Forschungsgemeinschaft (DFG grant no. INST 410/45-1 FUGG), and the Bavarian Research Network for Induced Pluripotent Stem Cells (ForIPS). JeW is a graduate student, and JW a member of the research training group 2162 "Neurodevelopment and Vulnerability of the Central Nervous System" of the Deutsche Forschungsgemeinschaft (DFG, German Research Foundation - 270949263/GRK2162). The authors gratefully acknowledge Georgia Minakaki for enriching discussions and Eliezer Masliah for providing A53T mice. In addition, the authors thank Holger Meixner and Ulrike Naumann for excellent technical support.

References

Amato, D., Natesan, S., Yavich, L., Kapur, S., Müller, C.P., 2011. Dynamic regulation of dopamine and serotonin responses to salient stimuli during chronic haloperidol treatment. Int. J. Neuropsychopharmacol. 14, 1327–1339.
Arango, V., Underwood, M.D., Mann, J.J., 2002. Serotonin brain circuits involved in major depression and suicide. Prog. Brain Res. 136, 443–453.
Ascoli, G.A., Alonso-Nanclares, L., Anderson, S.A., Barrionuevo, G., Benavides-Piccione, R., Burkhalter, A., Buzsáki, G., Cauli, B., Defelipe, J., Fairén, A., 2008. Petilla terminology: nomenclature of features of GABAergic interneurons of the cerebral cortex. Nat. Rev. Neurosci. 9, 557.
Azmitia, E.C., Nixon, R., 2008. Dystrophic serotonergic axons in neurodegenerative diseases. Brain Res. 1217, 185–194.
Barone, P., 2010. Neurotransmission in Parkinson's disease: beyond dopamine. Eur. J. Neurol. 17, 364–376.
Blesa, J., Trigo-Damas, I., Dileone, M., Del Rey, N., Hernandez, L.F., Obeso, J.A., 2017. Compensatory mechanisms in Parkinson's disease: circuits adaptations and role in disease modification. Exp. Neurol. 298 (Pt B), 148–161.
Braak, H., Del Tredici, K., Rüb, U., De Vos, R.A., Steur, E.N.J., Braak, E., 2003. Staging of brain pathology related to sporadic Parkinson's disease. Neurobiol. Aging 24, 197–211.
Burré, J., 2015. The synaptic function of α-synuclein. J. Parkinsons Dis. 5, 699–713.
Carter, O.L., Burr, D.C., Pettigrew, J.D., Wallis, G.M., Hasler, F., Vollenweider, F.X., 2005. Using psilocybin to investigate the relationship between attention, working memory, and the serotonin 1A and 2A receptors. J. Cogn. Neurosci. 17, 1497–1508.
Chen, L., Ding, Y., Cagniard, B., Van Laar, A.D., Mortimer, A., Chi, W., Hastings, T.G., Kang, U.J., Zhuang, X., 2008. Unregulated cytosolic dopamine causes neurodegeneration associated with oxidative stress in mice. J. Neurosci. 28, 425–433.
Cheng, H.C., Ulane, C.M., Burke, R.E., 2010. Clinical progression in Parkinson disease and the neurobiology of axons. Ann. Neurol. 67, 715–725.
Chu, Y., Morfini, G.A., Langhamer, L.B., He, Y., Brady, S.T., Kordower, J.H., 2012. Alterations in axonal transport motor proteins in sporadic and experimental Parkinson's disease. Brain 135, 2058–2073.
Chung, C.Y., Koprich, J.B., Siddiqi, H., Isacson, O., 2009. Dynamic changes in presynaptic and axonal transport proteins combined with striatal neuroinflammation precede dopaminergic neuronal loss in a rat model of AAV α-synucleinopathy. J. Neurosci. 29, 3365–3373.
Daws, L.C., Gould, G.G., Teicher, S.D., Gerhardt, G.A., Frazer, A., 2000. 5-HT1B receptor-mediated regulation of serotonin clearance in rat hippocampus in vivo. J. Neurochem. 75, 2113–2122.
Deusser, J., Schmidt, S., Ettle, B., Plötz, S., Huber, S., Müller, C.P., Masliah, E., Winkler, J., Kohl, Z., 2015. Serotonergic dysfunction in the A53T alpha-synuclein mouse model of Parkinson's disease. J. Neurochem. 135, 589–597.
Driver, J.A., Logroscino, G., Gaziano, J.M., Kurth, T., 2009. Incidence and remaining lifetime risk of Parkinson disease in advanced age. Neurology 72, 432–438.
Hagan, C.E., Mcdevitt, R.A., Liu, Y., Furay, A.R., Neumaier, J.F., 2012. 5-HT1B autoreceptor regulation of serotonin transporter activity in synaptosomes. Synapse 66, 1024–1034.
Halliday, G., Blumbergs, P., Cotton, R., Blessing, W., Geffen, L., 1990. Loss of brainstem serotonin-and substance P-containing neurons in Parkinson's disease. Brain Res. 510, 104–107.
Hashimoto, M., Rockenstein, E., Masliah, E., 2003. Transgenic models of α-synuclein pathology. Ann. N. Y. Acad. Sci. 991, 171–188.
Hawkes, C.H., 2008. The prodromal phase of sporadic Parkinson's disease: does it exist and if so how long is it? Mov. Disord. 23, 1799–1807.
Hornung, J.P., Fritschy, J.M., Törk, I., 1990. Distribution of two morphologically distinct subsets of serotoninergic axons in the cerebral cortex of the marmoset. J. Comp. Neurol. 297, 165–181.
Iversen, L., 2000. Neurotransmitter transporters: fruitful targets for CNS drug discovery. Mol. Psychiatry 5, 357.
Kelly, R.B., 1993. Storage and release of neurotransmitters. Cell 72, 43–53.
Kohl, Z., Winner, B., Ubhi, K., Rockenstein, E., Mante, M., Münch, M., Barlow, C., Carter, T., Masliah, E., Winkler, J., 2012. Fluoxetine rescues impaired hippocampal neurogenesis in a transgenic A53T synuclein mouse model. Eur. J. Neurosci. 35, 10–19.
Kohl, Z., Abdallah, N.B., Vogelgsang, J., Tischer, L., Deusser, J., Amato, D., Anderson, S., Müller, C.P., Riess, O., Masliah, E., 2016. Severely impaired hippocampal neurogenesis associates with an early serotonergic deficit in a BAC α-synuclein transgenic rat model of Parkinson's disease. Neurobiol. Dis. 85, 206–217.
Kosofsky, B.E., Molliver, M.E., 1987. The serotoninergic innervation of cerebral cortex: different classes of axon terminals arise from dorsal and median raphe nuclei. Synapse 1, 153–168.
Lavedan, C., 1998. The synuclein family. Genome Res. 8, 871–880.
Leenders, A.M., da Silva, F.H.L., Ghijsen, W.E., Verhage, M., 2001. Rab3a is involved in transport of synaptic vesicles to the active zone in mouse brain nerve terminals. Mol. Biol. Cell. 12, 3095–3102.
Linley, S.B., Hoover, W.B., Vertes, R.P., 2013. Pattern of distribution of serotonergic fibers to the orbitomedial and insular cortex in the rat. J. Chem. Neuroanat. 48, 29–45.
Liy-Salmeron, G., Meneses, A., 2008. Effects of 5-HT drugs in prefrontal cortex during memory formation and the ketamine amnesia-model. Hippocampus 18, 965–974.
Longair, M.H., Baker, D.A., Armstrong, J.D., 2011. Simple Neurite Tracer: open source software for reconstruction, visualization and analysis of neuronal processes. Bioinformatics 27, 2453–2454.
Masliah, E., Rockenstein, E., Veinbergs, I., Mallory, M., Hashimoto, M., Takeda, A., Sagara, Y., Sisk, A., Mucke, L., 2000. Dopaminergic loss and inclusion body formation in α-synuclein mice: implications for neurodegenerative disorders. Science 287, 1265–1269.
Molliver, M.E., Berger, U.V., Mamounas, L.A., Molliver, D.C., O'HEARN, E., Wilson, M.A., 1990. Neurotoxicity of MDMA and related compounds: anatomic studies. Ann. New York Acad. Sci. 600, 640–661.
Motulsky, H.J., Brown, R.E., 2006. Detecting outliers when fitting data with nonlinear regression–a new method based on robust nonlinear regression and the false discovery rate. BMC Bioinformatics 7, 123.
Muzerelle, A., Scotto-Lomassese, S., Bernard, J.F., Soiza-Reilly, M., Gaspar, P., 2016. Conditional anterograde tracing reveals distinct targeting of individual serotonin cell groups (B5–B9) to the forebrain and brainstem. Brain Struct. Funct. 221, 535–561.
Narboux-Nême, N., Sagné, C., Doly, S., Diaz, S.L., Martin, C.B., Angenard, G., Martres, M.-P., Giros, B., Hamon, M., Lanfumey, L., 2011. Severe serotonin depletion after conditional deletion of the vesicular monoamine transporter 2 gene in serotonin neurons: neural and behavioral consequences. Neuropsychopharmacology 36, 2538.
Nayyar, T., Bubser, M., Ferguson, M.C., Diana Neely, M., Shawn Goodwin, J., Montine, T.J., Deutch, A.Y., Ansah, T.A., 2009. Cortical serotonin and norepinephrine denervation in parkinsonism: preferential loss of the beaded serotonin innervation. Eur. J. Neurosci. 30, 207–216.
Nemani, V.M., Lu, W., Berge, V., Nakamura, K., Onoa, B., Lee, M.K., Chaudhry, F.A., Nicoll, R.A., Edwards, R.H., 2010. Increased expression of α-synuclein reduces neurotransmitter release by inhibiting synaptic vesicle reclustering after endocytosis. Neuron 65, 66–79.
Nuber, S., Harmuth, F., Kohl, Z., Adame, A., Trejo, M., Schönig, K., Zimmermann, F., Bauer, C., Casadei, N., Giel, C., 2013. A progressive dopaminergic phenotype associated with neurotoxic conversion of α-synuclein in BAC-transgenic rats. Brain 136, 412–432.
Paulus, W., Jellinger, K., 1991. The neuropathologic basis of different clinical subgroups of Parkinson's disease. J. Neuropathol. Exp. Neurol. 50, 743–755.
Paxinos, G., Franklin, K., 2012. Paxinos and Franklin's the Mouse Brain in Stereotaxic Coordinates; 4th Edition.
Politis, M., Wu, K., Loane, C., Kiferle, L., Molloy, S., Brooks, D.J., Piccini, P., 2010. Staging of serotonergic dysfunction in Parkinson's disease: an in vivo 11C-DASB PET study. Neurobiol. Dis. 40, 216–221.
Riad, M., Garcia, S., Watkins, K.C., Jodoin, N., Doucet, É., Langlois, X., El Mestikawy, S., Hamon, M., Descarries, L., 2000. Somatodendritic localization of 5-HT1A and preterminal axonal localization of 5-HT1B serotonin receptors in adult rat brain. J. Comp. Neurol. 417, 181–194.
Riga, D., Matos, M.R., Glas, A., Smit, A.B., Spijker, S., Van den Oever, M.C., 2014. Optogenetic dissection of medial prefrontal cortex circuitry. Front. Syst. Neurosci. 8, 230.
Rizzoli, S.O., 2014. Synaptic vesicle recycling: steps and principles. EMBO J. 33, 788–822.
Rockenstein, E., Hansen, L.A., Mallory, M., Trojanowski, J.Q., Galasko, D., Masliah, E., 2001. Altered expression of the synuclein family mRNA in Lewy body and Alzheimer's disease. Brain Res. 914, 48–56.
Sasahara, A., Kott, J.N., Sasahara, M., Raines, E.W., Ross, R., Westrum, L.E., 1992. Platelet-derived growth factor B-chain-like immunoreactivity in the developing and adult rat brain. Developmental Brain Res. 68, 41–53.
Scatton, B., Javoy-Agid, F., Rouquier, L., Dubois, B., Agid, Y., 1983. Reduction of cortical dopamine, noradrenaline, serotonin and their metabolites in Parkinson's disease. Brain Res. 275, 321–328.
Tagliaferro, P., Burke, R.E., 2016. Retrograde axonal degeneration in Parkinson disease. J. Parkinsons Dis. 6, 1–15.
Vale, R.D., 2003. The molecular motor toolbox for intracellular transport. Cell 112, 467–480.
Van Luijtelaar, M., Steinbusch, H., Tonnaer, J., 1989. Similarities between aberrant serotonergic fibers in the aged and 5, 7-DHT denervated young adult rat brain. Exp. Brain Res. 78, 81–89.
Walther, D.J., Peter, J.U., Bashammakh, S., Hörtnagl, H., Voits, M., Fink, H., Bader, M., 2003. Synthesis of serotonin by a second tryptophan hydroxylase isoform. Science 299, 76.
Wilson, M., Molliver, M., 1991. The organization of serotonergic projections to cerebral cortex in primates: regional distribution of axon terminals. Neuroscience 44, 537–553.
Winner, B., Rockenstein, E., Lie, D.C., Aigner, R., Mante, M., Bogdahn, U., Couillard-Despres, S., Masliah, E., Winkler, J., 2008. Mutant α-synuclein exacerbates age-related decrease of neurogenesis. Neurobiol. Aging 29, 913–925.